

Paper:

Fabrication of SiO₂-ZnO Core-Shell Urchin-Like Structure by Hydrothermal Method Using Self-Assembled Particles as Nuclei and Application to UV-Activated Gas Sensors

Daiki Funakawa[†] and Nobuyuki Moronuki

Tokyo Metropolitan University

6-6 Asahigaoka, Hino-shi, Tokyo 191-0065, Japan

[†]Corresponding author, E-mail: microfd@outlook.jp

[Received June 12, 2019; accepted October 23, 2019]

This study aims to improve the efficiency of gas sensors with a zinc oxide (ZnO) structure by widening the surface area for reaction and using UV-activation. The silica (SiO₂)-ZnO core-shell urchin-like structure is a promising candidate to achieve this aim, due to its broad surface area and electrically insulated formation. The higher resistivity of silica prevents the escape of electrons and recombination during reaction with gas; thus, improving its sensitivity. The structure was fabricated by a two-step process. First, ZnO-silica core-shell structures were produced. ZnO nanoparticles ($\phi \leq 34$ nm) self-assembled to form a shell around a core comprising silica particles ($\phi 5 \mu\text{m}$). Gravity sedimentation was then used to obtain the silica particles, while the ZnO particles were obtained by dropping and drying of the suspension. Closely packed structures were obtained due to the meniscus attraction between the particles at the drying stage of the suspension. Second, ZnO urchin-like structures were synthesized on the silica particles using the hydrothermal method, with the originally placed ZnO nanoparticles as the nuclei. The method is a simple material synthesis involving the crystal growth process in a sealed container, in which substrates and precursors are stored and maintained at an elevated temperature. The obtained structure (or morphology) changed depending on the nucleation and growth conditions. The appropriate conditions were clarified through systematic experiments. Finally, the gas sensor performance was examined.

Keywords: ZnO, core-shell, hydrothermal method, gas sensor, UV activation

1. Introduction

ZnO is a superior gas sensor material because it has excellent semiconducting properties (as required for gas sensors) such as a wide bandgap energy (3.37 eV) and large excitation binding energy (60 mV) [1]. It also has many advantages such as low cost, being harmless, long-

term stability, and simplicity of morphology control by changing the conditions of the crystal growth [2–3].

The working principle is the resistance change of the structure due to the electron exchange at the surface with gas molecules [4]. Thus, the sensing performance can be improved by widening the surface area. However, a higher energy consumption is inevitable, because heating to approximately 300°C is required to achieve sufficient sensitivity. To solve this problem, UV with a higher photon energy than the bandgap energy of ZnO can be an alternative option [5–10]. With the irradiation of UV, electron-hole pairs are excited, and then active adsorbed oxygen (which enhances the reaction) is generated. However, the sensitivity was lower than that using heat activation, because the excited procedure cannot be used efficiently.

Combining SiO₂ and ZnO can improve the efficiency because the higher insulation property of SiO₂ prevents the escape of electrons, and active oxygen will be efficiently produced [11–13]. In addition, if a wider surface area of the ZnO structure (such as rod- or urchin-shaped) is regularly placed, the sensitivity and the efficiency will be significantly increased.

In previous studies, ZnO micro-urchin structures [14] and hollow sphere structures [15] were fabricated by the hydrothermal process, using self-assembled particles as nuclei. This process is a simple crystal growth process in a sealed container in which precursors are stored and kept at an elevated temperature. The structure is then fabricated in the positions of the particles.

In this study, SiO₂-ZnO core-shell urchin like structures were fabricated, extending previous studies of the ZnO hydrothermal method, and the gas sensing characteristics were examined. Herein, the term “core-shell urchin-like structure” signifies ZnO rods placed perpendicular to SiO₂ spherical cores.

2. Hydrothermal Method

2.1. Principle

The hydrothermal method is a synthesis method for growing single crystals from an aqueous solution in an



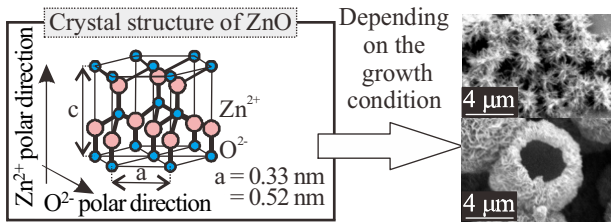


Fig. 1. Crystal structure of ZnO.

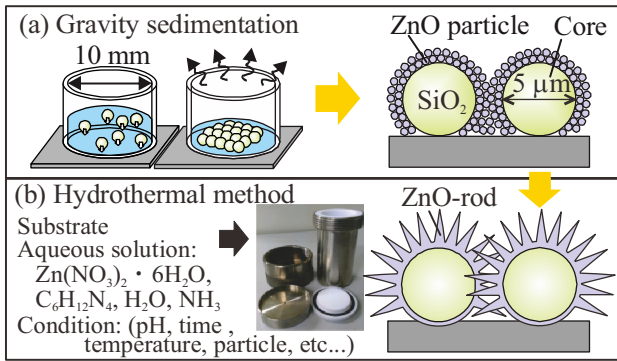


Fig. 2. Proposed process of this study. (a) Gravity sedimentation. (b) Hydrothermal method.

autoclave (a thick-walled and sealed vessel) at high temperature and pressure. The procedure involves placing source material solutions in an autoclave and maintaining a specified temperature for a specific time. Usually, crystal growth based on the crystal structure will occur, however, changing the conditions of the growth or nucleation will in turn change the obtained structure.

Figure 1 shows the hexagonal crystal structure of ZnO. A rod-like structure is often obtained because the selective growth proceeds along the *c*-axis due to the difference in the surface energy of the facets. When a substrate is placed in the autoclave, the crystal growth and thus the structural morphology can be controlled. Location-selective growth is also possible by placing the same material as a nuclei at the required position before the hydrothermal process [16].

2.2. Fabrication of Core-Shell Urchin-Like Structure

Figure 2 shows the two-step process used in this study. To obtain the core-shell urchin-like structure, the rod-like growth of ZnO on individual SiO₂ particle surfaces is necessary. In this study, ZnO nanoparticles were used as the nuclei, similar to our previous study [14, 15].

First, ZnO-silica core-shell structures were produced. ZnO nanoparticles ($\phi \leq 34$ nm), which served as the nuclei, were self-assembled to form a shell on the silica-particles ($\phi 5 \mu\text{m}$) core. Gravity sedimentation [17] was used for the silica particles, and the process of dropping and drying the suspension was used for the ZnO particles. Closely packed structures were obtained due to the menis-

Table 1. Gravity sedimentation conditions.

Silica suspension	Solvent	Pure water
	Particle	SiO ₂ , $\phi 5 \mu\text{m}$
	Concentration	0.3 wt. %
ZnO suspension	Solvent	Pure water
	Particle	ZnO, $\phi \leq 34$ nm
	Concentration	0.3 wt. %
Drop volume		150 μL
Substrate	Si/PDMS 1.5 × 1.5 cm O ₂ plasma (2 min)	

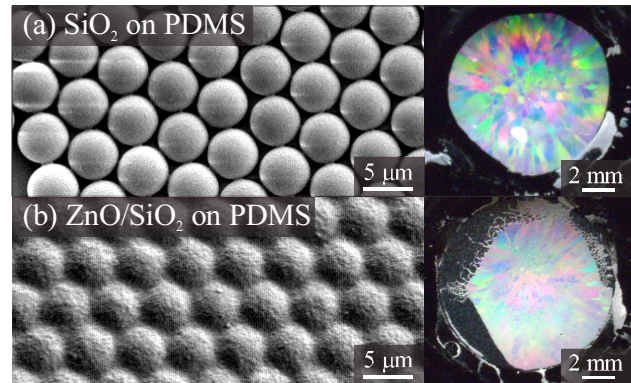
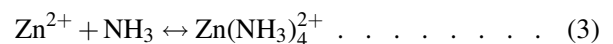
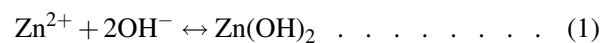


Fig. 3. Results of gravity sedimentation. (a) SiO₂. (b) ZnO on SiO₂ (core-shell).

cus attraction between the particles at the drying stage of suspension. Table 1 shows the conditions for the core-shell structure and Fig. 3 shows the SEM images of the cores and core-shell structures. A silicon substrate, on which polydimethylsiloxane (PDMS; Sylgard 184) was spun-coated (1 μm), was used. The low elastic modulus of the PDMS helped keep the particles on the substrate during the hydrothermal process because of the wide contact area.

Second, the core-shell urchin-like structure was fabricated using a rod-like growth of ZnO by the hydrothermal method, using the shell structure as the nuclei. Eqs. (1)–(6) show the chemical reaction that proceeded in the autoclave as well as the way the ZnO was supplied for the crystal growth [18–20].



The complex and reversible chemical reactions that proceed in parallel make the estimation of the final structures difficult. Thus, appropriate conditions for the fab-

Table 2. Hydrothermal conditions.

Material composition	Zn(NO ₃) ₂ ·6H ₂ O : C ₆ H ₁₂ N ₄	4 : 4 mM
	Water	30 mL
	pH	6.3, 8, 11
Hydrothermal condition	Temperature	150°C
	Reaction time	13 h

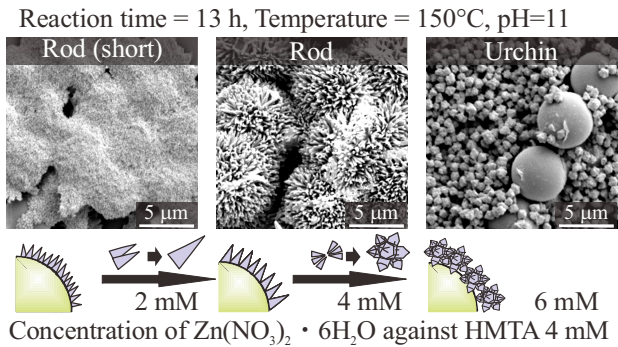


Fig. 4. Influence of Zn(NO₃)₂ · 6H₂O concentration on morphology.

rication and the influence of the conditions (i.e., particles, pH, concentration of zinc, reaction time, and temperature) on the ZnO morphology require investigation by a systematic experiment. The typical conditions are summarized in **Table 2**. The source materials for the synthesis were a mixture of zinc nitrate hexahydrate (Zn(NO₃)₂·6H₂O), hexamethylene-tetramine (HMTA, C₆H₁₂N₄), and ultra-pure water. An NH₃ solution was added to control the pH as this affects the reaction process. The source materials and the substrate were placed into an autoclave (Teflon-sealed, capacity 50 mL) and maintained at a specified temperature for a specific duration.

3. Result

3.1. Influence of Zn(NO₃)₂·6H₂O Concentration

To investigate the influence of the Zn²⁺ ions on the morphology of the synthesized ZnO, hydrothermal reactions were conducted with different concentrations of Zn(NO₃)₂·6H₂O (2, 4, and 6 mM), which served as the source of Zn²⁺. **Fig. 4** shows the results. When the concentration was 4 mM or less, rod-like structures were observed on the silica particles. This structure is different from the urchin-like structure because the rods are separated, while those in the urchin-like structure are interconnected at one end. With the increase of Zn²⁺, the rod height also increased (2 mM: 0.1 μm, 4 mM: 1.3 μm). When the concentration exceeded 6 mM, urchin-like ZnO structures, which resemble an assembly of rods, were fabricated and the silica particles peeled off. The growth of the rods was found to be enhanced with higher concen-

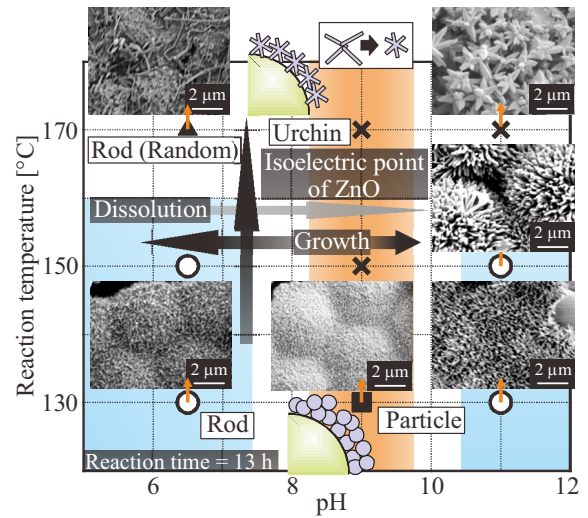


Fig. 5. Influence of pH and reaction temperature on morphology.

trations of Zn²⁺; however, the aggregation of rods was also promoted. Considering the balance of these effects, the concentration of Zn(NO₃)₂·6H₂O was determined as 4 mM for the following experiments.

3.2. Influence of pH and Reaction Temperature

Figure 5 shows the influence of the pH and reaction temperature on the morphology. In this case, the obtained structures were divided into four categories (○: Rod, ▲: Rod (Random), ■: Particle, ×: Urchin). The points are summarized as follows.

- 1) Comparing the results of the different pH values at 130°C, particle-like shapes were obtained at pH 9, while rod structures were obtained otherwise. The isoelectric point of ZnO is at approximately pH 8.5–9.5, and the bias is small in this range. However, away from the isoelectric point, the difference in the electrical potential will change the collecting of ions. Thus, the anisotropy became strong.
- 2) At 150°C, rods with heights of approximately 1.3 μm were obtained at pH 11, while a height of approximately 0.4 μm was obtained at pH 6.5. The pH was adjusted by the NH₃ concentration; it is thought that the decomposition of ZnO was promoted at high pH.
- 3) At temperatures above 170°C, connected rod structures were obtained. This suggests that while the reaction rate was enhanced with the temperature rise, the reaction promoted fusion at high zinc nitrate concentrations. In addition, although the pH was as low as 6.5, the tips of the rods were connected to each other. This suggests that positive polarity predominates at a pH lower than the isoelectric point of ZnO, which may promote the recombination reaction between Zn²⁺ polar faces. The detailed formation mechanism is difficult to identify from these results because

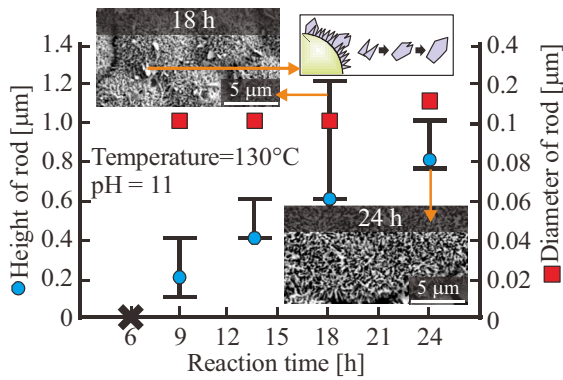


Fig. 6. Influence of reaction time on morphology.

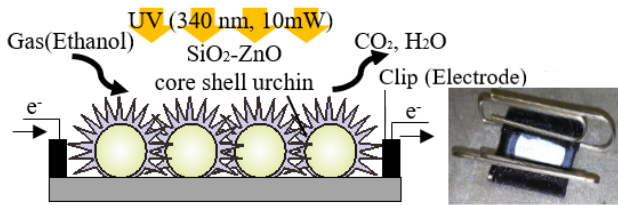


Fig. 7. Schematic of gas sensor test with UV irradiation.

the effects of the temperature and pH are not considered as independent.

From these results, it is considered that low temperature and high pH are suitable for producing the target structure; hence, in the following, the conditions of 130°C and pH 11 were adopted.

3.3. Influence of Reaction Time

Figure 6 shows the influence of the reaction time on the morphology. The reaction time was varied while the temperature and pH were constant, at 130°C and pH 11, respectively, and the effect was investigated. It was found that the rod length could be controlled with the reaction time, while the diameter of the rod remained almost constant at around 0.1 μm. For a reaction time of 18 h, the variation in length became large and appeared as a pentagonal disk shape. It is suggested that the rods were connected by O²⁻ polar surfaces [21]. As the pH was higher than the isoelectric point of ZnO, negative polarity is considered to have been dominant; thus, promoting the merging reaction.

4. Application to Gas Sensor

4.1. Sensor Fabrication and Sensing Measurements

A schematic of the experiment is shown in Fig. 7. Conductive-adhesive tapes and clips were set as the electrodes at both edges of the substrate. Insulation adhesive tapes were placed on the backside to eliminate the effect of conduction through the substrate. The resistance

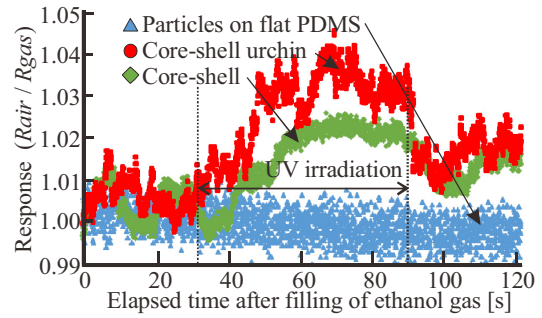


Fig. 8. Gas sensor response under UV irradiation showing the effect of different structures.

Table 3. Gravity sedimentation conditions for comparison.

ZnO suspension	Solvent	Pure water
	Particle	ZnO, φ100 nm
	Concentration	10 wt.%
	Drop volume	150 μL

was measured with an LCR meter (HIOKI, 3511-50) of four-terminal probes, and UV irradiation was introduced with a UV source (SUMICA, LS-165UV). The whole system was installed in a chamber (400 mm × 800 mm × 600 mm). During the experiments, the chamber was filled with ethanol gas (1,000 ppm), of liquid ethanol vapor. Before and after the test, the gas concentration was calibrated with an authorized gas detecting tube (GASTEC).

4.2. Sensing Performance

The gas sensitivity under UV irradiation (340 nm, 10 mW) was examined without temperature rise. To investigate the effect of morphology difference, comparative experiments of the core-shell urchin-like (height of ~0.8 μm) and core-shell (before hydrothermal reaction) structures, and ZnO particle assembly (φ ≤ 34 nm) were carried out. Fig. 8 shows the result. A response was observed during UV irradiation 30–90 s after starting the measurement. The vertical axis shows the response, which was calculated by dividing the resistance without gas by that in gas, and the larger the response, the better. The gas was undetectable when the structure comprised assembled ZnO particles only. The response increased to approximately 1.02 with the core-shell structure and to approximately 1.04 with the core-shell urchin-like structure. Comparing these results, the influence of the SiO₂ core is clear, and the effect of the surface area increase with the urchin-like structure is also clear.

4.3. Influence of Resistivity of the Substrates

The sensitivity improvement by the SiO₂ core was confirmed from Fig. 8, but its cause cannot be identified. To investigate the influence of the core material resistance, ZnO particles of 100 nm were assembled by gravity sedimentation under the conditions of Table 3 on the substrates with different resistivities (glass (SiO₂), PDMS,

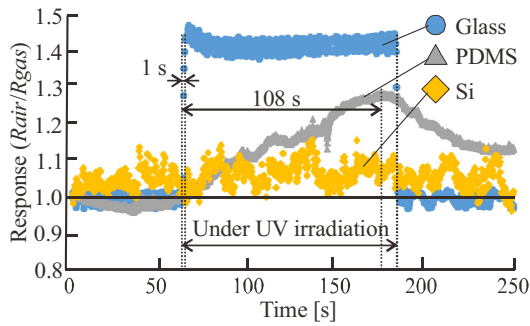


Fig. 9. Influence of insulation material on sensor property.

Table 4. Summary of sensor properties.

Substrate	Si	PDMS	Glass [22]
Resistivity [$\Omega \cdot \text{cm}$]	1–20	7×10^{11}	10^{14}
Resistance R_{air} [$10^5 \Omega$]	2.26	2.50	1760
R_{air} under UV [$10^5 \Omega$]	1.90	1.90	1240
Response R_{air}/R_{gas}	1.15	1.28	1.45
Response time T_{rsp} [s]	–	120	1
Recovery time T_{rcv} [s]	–	–	1

and Si). Fig. 9 shows the responses of the sensors and the results are summarized in Table 4.

In the case of glass, the response was quick and the sensitivity was the highest. The results are also shown for the case of PDMS, in which the time response was slow, and it did not return to the original resistance value, particularly after irradiation. Additionally, the Si substrate showed almost no response. As the substrate resistivity increases in the order of glass > PDMS > Si, it is believed that the high resistivity prevents the flow of electrons to the substrate. Furthermore, the high resistivity of SiO₂ was confirmed to be effective for improving the gas sensitivity.

4.4. Influence of Surface Area on Sensing Performance

An increase in the surface area is preferable because the gas adsorption increases. Therefore, to clarify the influence of the structure, it is desirable to compare the sensitivity per surface area. The surface area (S_{ZT}) of the core-shell urchin-like structure used was estimated as follows: assuming that the SiO₂ particles of radius (R) are closely packed (74%) in the area ($S_A = 47.1 \text{ mm}^2$) to be precipitated, S_{ZT} is given by:

$$S_{ZT} = \frac{0.74S_A}{\pi R^2} \times S_Z \dots \dots \dots (7)$$

where S_Z indicates the surface area of the ZnO structure per SiO₂ particle, and it is derived assuming that the rod structures, with radius $r = 0.15 \mu\text{m}$ and height $h = 0.8 \mu\text{m}$, are closely packed on the surface of SiO₂ (Eq. (8)).

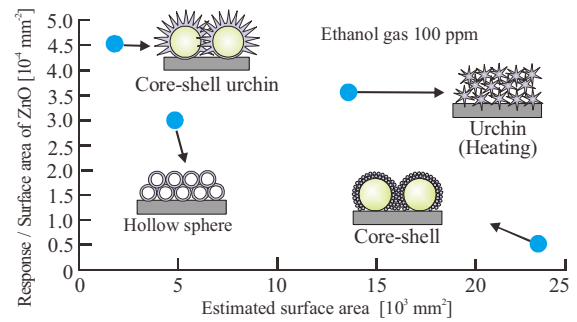


Fig. 10. Response per surface area for different structures.

Table 5. Summary of sensor properties.

Structure	Surface area [mm^2]	Maximum response	Response / surface area
Core-shell urchin	2.34×10^3	1.05	4.48×10^{-4}
Core-shell	2.34×10^4	1.03	4.39×10^{-5}
Hollow sphere	5.00×10^3	1.40	2.8×10^{-4}
Urchin (heating)	1.24×10^4	4.00	3.22×10^{-4}

$$S_Z = \frac{0.74 \times 4\pi R^2}{\pi r^2} \times (\pi r^2 + 2\pi rh) \dots \dots \dots (8)$$

The comparison results are summarized in Fig. 10 and Table 5, and it can be seen that the proposed structure has a high sensitivity per area.

In the case of the core-shell structure, it is assumed that the gas could not diffuse inside the layered structure of the particles; thus, the efficiency was low. Diffusion may be the dominant factor in this case. A hollow sphere structure with an air core whose resistivity is expected to be similar to that of SiO₂ is also expected to have high efficiency, but the result was low efficiency. It is believed that electrons were trapped at the SiO₂ interface, which is different from gas, and that the resistivity of air was lowered by the wet environment.

An issue to examine in future is the low maximum sensitivity. As the surface area is smaller than that of other structures, it is considered effective to increase the surface area, such as lengthening the rod.

5. Conclusions

This study is summarized as follows.

- 1) The effects of conditions such as the core particle, zinc nitrate concentration, pH, reaction temperature, and reaction time on the hydrothermal synthesis were clarified. Core-shell urchin-like structures were produced with controlled rod length.
- 2) The effect of the structure on the gas sensor sensitivity was confirmed.

References:

- [1] L. Wang, Y. Kang, X. Liu, S. Zhang, W. Huang, and S. Wang, "ZnO nanorod gas sensor for ethanol detection," *Sensor and Actuators, B*, Vol.162, pp. 237-243, 2012.
- [2] J. Zhang, W. X. Que, Q. Jia, and X. Ye, "Controllable hydrothermal synthesis of ZnO nanowires arrays on Al-doped ZnO seed layer and patterning of ZnO nanowires arrays via surface modification of substrate," *Applied Surface Science*, Vol.257, pp. 10134-10140, 2011.
- [3] R. Shi, P. Yang, X. Song, and J. Wang, "ZnO flower: Self-assembly growth from nanosheets with exposed {1100} facet, white emission, and enhanced photocatalysis," *Applied Surface Science*, Vol.366, pp. 506-513, 2016.
- [4] Z. Guo, G. Chen, G. Zheng, L. Liu, and C. Zhang, "Metal oxides and metal salt nanostructures for hydrogen sulfide sensing: mechanism and sensing performance," *RSC Adv.*, Vol.67, pp. 54793-54805, 2015.
- [5] M. Procek, A. Stolarczyk, and T. Pustelny, "Impact of Temperature and UV irradiation on Dynamics of NO₂ Sensors Based on ZnO Nanostructure," *Nanomaterials*, Vol.7, p. 312, 2017.
- [6] Y. Chen, X. Li, J. Wang, and Z. Tang, "UV activated hollow ZnO microspheres for selective ethanol sensors at low temperature," *Sensors and Actuators, B*, Vol.233, pp. 158-164, 2016.
- [7] H. Chen, Y. Liu, C. Xie, J. Wu, D. Zeng, and Y. Liao, "A comparative study on UV light activated porous TiO₂ and ZnO film sensors for gas sensing at room temperature," *Ceramics Int.*, Vol.38, No.1, pp. 503-509, 2012.
- [8] S. W. Fan, A. K. Srivastava, and V. P. Dravid, "UV-activated room-temperature gas sensing mechanism of polycrystalline ZnO," *Appl. Phys. Lett.*, Vol.95, 142106, 2009.
- [9] J. Cui, J. Jiang, L. Shi, F. Zhao, D. Wang, Y. Lin, and T. Xie, "The role of Ni doping on photoelectric gas-sensing properties of ZnO nanofibers," *RSC Adv.*, Vol.6, pp. 78257-78263, 2016.
- [10] P. Zhang, G. Pan, J. Zhen, and Y. Sun, "High sensitivity ethanol gas sensor based on Sn-doped ZnO under visible light irradiation at low temperature," *Mat. Res.*, Vol.17, No.4, pp. 817-822, 2014.
- [11] N. A. Galedari, M. Rahmani, and M. Tabihi, "Preparation, characterization, and application of ZnO@SiO₂ core-shell structured catalyst for photocatalytic degradation of phenol," *Environ Sci. Pollut. Res.*, Vol.24, No.14, pp. 12655-12663, 2017.
- [12] C. Y. Huang, Y. J. Yang, J. Y. Chen, C. H. Wang, Y. F. Chen, L. S. Hong, C. S. Liu, and C. Y. Wu, "p-Si nanowires/SiO₂/n-ZnO heterojunction photodiodes," *Appl. Phys. Lett.*, Vol.97, 013503, 2010.
- [13] J. W. Lee, M. R. Othman, Y. Eom, T. G. Lee, W. S. Kim, and J. Kim, "The effects of sonification and TiO₂ deposition on the micro-characteristics of the thermally treated SiO₂/TiO₂ spherical core-shell particles for photo-catalysis of methyl orange," *Microporous and Mesoporous Materials*, Vol.116, Issues 1-3, pp. 561-568, 2008.
- [14] N. Moronuki and Y. Okubo, "Self-assembly of ZnO particles and subsequent hydrothermal crystal growth to produce ZnO urchin-like structure and its application to gas sensor," *J. of JSPE*, Vol.84, No.3, pp. 267-271, 2018.
- [15] D. Funakawa and N. Moronuki, "Production of ZnO regular microstructure by hydrothermal process with controlled nucleation aiming at efficient gas sensor," *Proc. of 17th Int. Conf. on Precision Engineering (ICPE2018)*, F-2-6, 2018.
- [16] N. Moronuki, "Hydrothermal synthesis with controlled nucleation and growth to produce regular structures," *euspen's 18th Int. Conf. & Exhibition*, p. 397, 2018.
- [17] W.-S. Chae, D. V. Gough, S.-K. Han, D. B. Robinson, and P. V. Braun, "Effect of Ordered Intermediate Porosity on Ion Transport in Hierarchically Nanoporous Electrodes," *ACS Appl. Mater. Inter.*, Vol.4, Issue 8, pp. 3973-3979, 2012.
- [18] A. Wei, X. W. Sun, C. X. Xu, Z. L. Dong, Y. Yang, S. T. Tan, and W. Huang, "Growth mechanism of tubular ZnO formed in aqueous solution," *Nanotechnology*, Vol.17, p. 1740, 2006.
- [19] S. Cho, J. W. Jang, S. H. Jung, B. R. Lee, E. Oh, and K. H. Lee, "Precursor effect of Citric Acid and Citrates on ZnO Crystal Formation," *Langmuir*, Vol.25, No.6, pp. 3825-3831, 2009.
- [20] Y. F. Zhu, D. H. Fan, and W. Z. Shen, "Template-Free Synthesis of Zinc Oxide Hollow Microspheres in Aqueous Solution at Low Temperature," *J. Phys. Chem., C*, Vol.111, pp. 18629-18635, 2007.
- [21] K. S. Kim, H. Jeong, M. S. Jeong, and G. Y. Jung, "Polymer-Templated Hydrothermal Growth of Vertically Aligned Single-Crystal ZnO Nanorods and Morphological Transformations Using Structural Polarity," *Adv. Func. Mater.*, Vol.20, pp. 3055-3063, 2010.
- [22] G. Gamov, "Matter, Earth, and Sky," Prentice Hall, 1965.

**Name:**

Daiki Funakawa

Affiliation:

Tokyo Metropolitan University

Address:

6-6 Asahigaoka, Hino, Tokyo 191-0065, Japan

Brief Biographical History:

2019 Received Master degree from Tokyo Metropolitan University

Membership in Academic Societies:

- Japan Society for Precision Engineering (JSPE)

**Name:**

Nobuyuki Moronuki

Affiliation:

Professor, Tokyo Metropolitan University

Address:

6-6 Asahigaoka, Hino, Tokyo 191-0065, Japan

Brief Biographical History:

1989 Received Doctoral degree from Tokyo Metropolitan University

1990- Associate Professor, Tokyo Metropolitan University

2005- Professor, Tokyo Metropolitan University

Main Works:

- "Combination of silicon microstructures and porous cellulose nanofiber structures to improve liquid-infused-type self-cleaning function," *Precision Engineering*, Vol.51, pp. 638-646, 2018.

Membership in Academic Societies:

- Japan Society of Mechanical Engineers (JSME)
- Japan Society for Precision Engineering (JSPE)
- European Society for Precision Engineering and Nanotechnology (euspen)